

## Reference Values of Myocardial T1 Relaxation Times in Healthy Latin American Patients

Nelsy Gonzalez Ramirez<sup>1\*</sup>, Brenda Caroline Fountains Lopez<sup>1</sup>, A.S. Caesar Nicholas Christian Rojas<sup>1</sup>, A.S. Yuki Yoshi Kimura Fujikami<sup>1</sup>, Keyra Miroslava<sup>5</sup>

<sup>1</sup>Head of Cardiovascular Imaging CT Scanner Mexico.

**\*Corresponding Author:**

Nelsy Gonzalez Ramirez, Head of Cardiovascular Imaging CT Scanner Mexico.

Submitted: 04 Jan 2023; Accepted: 17 Jan 2023; Published: 03 Feb 2023

**Citation:** Ramirez N. G, Lopez B. C. F, Rojas A.S.C.N.C, Fujikami A. S. Y.K, Miroslava K. (2023). Reference Values of Myocardial T1 Relaxation Times in Healthy Latin American Patients, *J Nur Healthcare*, 8(1), 67-78.

**Abstract**

*Theoretical framework. Cardiac magnetic resonance imaging (CMR) is an invaluable tool for diagnosis and risk stratification in a broad spectrum of cardiac diseases. Magnetic resonance imaging techniques are increasingly complemented by mapping sequences that allow quantitative assessment of myocardial tissue with measurement of absolute relaxation times T1, T2, and T2\*. The clinical utilities are diverse, among which is the quantification of edema and/or fibrosis through the estimation of the extracellular volume fraction calculated from pre-contrast, post-contrast and hematocrit T1 relaxation times. There are multiple ways to obtain T1 mapping images, among which the modified look-locker inversion recovery technique (MOLLI) stands out. However, different manufacturers have designed various methods of obtaining them with slight variability between the equipment.*

**Aim**

*To determine the reference values of myocardial T1 relaxation times in our population to justify their clinical interpretation in the tissue evaluation of different cardiovascular diseases.*

**Material and method.**

*Type of study: prospective observational and single center.*

**Field intensity/sequence**

*A short CMR protocol was performed in a 1.5 T resonator, using the MOLLI technique, in T1 mapping.*

**Evaluation**

*Global and segmental T1 values were quantified, using the American Heart Association (AHA) model, for the entire left ventricle, in three short-axis slices (basal, mid, and apical). The post processing and analysis of the data with the commercialized software, Cvi42.*

**Results**

*The mean global myocardial T1 value was 1069.41 ms with a SD of 38.73 msec. Among the age groups, the <34-year-old group had the lowest global T1 values (1057 SD 33 msec), and the 35-year-old group -44 years obtained the highest values (1100 SD 50 msec), so no relationship was found between the linear increase in age and the variability of relaxation times. Between both sexes, men had lower global T1 values than women (1049 vs 1086).*

**conclusions**

*Native T1 ranges can serve as a basis for the quantitative characterization of the myocardium in the context of focal or diffuse diseases, in patients with infarcts, storage diseases, and inflammatory diseases. We are getting closer to standardizing the clinical use of these techniques by CMR. In conclusion, this analysis allows us to take another step to establish their use in the Latin American population.*

**Introduction**

Advances in CMR have allowed not only anatomical and functional evaluation, but it is also considered the reference imaging

modality for myocardial tissue characterization. The evaluation of the myocardium is based on the relative changes in signal intensity between the abnormal and normal myocardium. It is usually

---

performed qualitatively or semi-quantitatively, which can cause difficulties and limitations, especially in diffuse myocardial processes, since there is no reference normal myocardium at the time the images are obtained.

In the last decade, parametric mapping techniques have emerged, allowing rapid tissue characterization based on absolute quantifiable differences in T1 longitudinal and T2 transverse magnetization recovery rates [1, 2].

A T1 map is an image in which the signal intensity of each voxel is directly proportional to the T1 time of the tissue in which it is located. Unlike T1-weighted images, mapping allows visualization and quantification of the disease process regardless of whether it is focal or diffuse. This is important because historically, diffuse myocardial disease has been difficult to appreciate and quantify non-invasively [2].

T1 mapping techniques performed with or without contrast allow the quantification of diffuse myocardial fibrosis and myocardial infiltration. Myocardial edema and inflammation can be assessed with T2 mapping techniques. T2\* provides an assessment of myocardial iron overload and myocardial hemorrhage [3].

T1 mapping sequences employ different techniques to acquire a series of images at different inversion times, from which a T1 recovery curve is generated. This can be done by repeat acquisitions with various inversion-recovery times. Sequences have been designed in which all the necessary acquisitions are made in a single apnea and in the same phase of the cardiac cycle. The first of these, developed in 2004, is called modified look-locker inversion-recovery (MOLLI). Several modifications of the MOLLI sequence and other alternative approaches have been proposed as a shortened version (shMOLLI) that allows to reduce the apnea time [2-4].

There are various studies that have published reference values for the quantitative analysis of the myocardium, however, in our country and in the rest of Latin America, to our knowledge, these values do not currently exist. reference, which are necessary for clinical use according to the recommendations that the Cardiovascular Magnetic Resonance Society (SCMR) and the European Association of Cardiovascular Imaging (EACVI) published in 2017 [5-8]. In this sense, we consider it necessary to determine the reference values of our population, to justify its clinical interpretation in the tissue evaluation of the different cardiovascular pathologies.

### **Theoretical Framework myocardial fibrosis**

The extracellular matrix of the myocardium is composed of a complex number of macromolecules, including collagen proteins. Thus, in the myocardium there are type I, III and IV fibers, with type I (80%) and type III (10%) being predominant [9]. The collagen matrix plays an essential role in providing strength to the myocardium, as well as in creating an intercellular communication matrix. Increased myocardial collagen deposition is the common

endpoint in a wide variety of cardiomyopathies and results in abnormal myocardial hardness and contractility that eventually progresses to heart failure and disruption of the intercellular communication network, which can result in malignant arrhythmias. and sudden cardiac death [10].

Myocardial fibrosis is defined as a significant increase in the volume fraction of collagen in the myocardial tissue, and is always found in end-stage heart disease. Diffuse myocardial fibrosis has even been seen to occur as part of the aging process, but its appearance is accelerated in the disease. An increase in the amount of collagen in the myocardial tissue is the result of an alteration in the collagen renewal processes, in which the deposit exceeds its degradation [4]. The distribution of fibrosis varies according to the underlying pathology, which is why there are sometimes discrepancies in the pathology reports. Molecular mechanisms vary with different diseases, are complex, and are currently not fully understood [11]. The progressive accumulation of collagen conditions a spectrum of ventricular dysfunction processes that commonly affect diastole initially and subsequently systole. There are various types of fibrosis depending on the cardiomyopathic process; They can be divided into two large groups: interstitial fibrosis and replacement fibrosis [12, 13].

### **Interstitial Fibrosis**

It presents a diffuse pattern and includes reactive interstitial fibrosis and infiltrative interstitial fibrosis. Eventually both types of fibrosis lead to cardiomyocyte apoptosis and replacement fibrosis [4].

### **Reactive Interstitial Fibrosis**

This type of fibrosis presents a diffuse interstitial pattern but may also have a perivascular predominance. It presents progressively due to the increase in collagen synthesis and deposition by myofibroblasts under the influence of different stimuli. It has been described mainly in hypertension and diabetes mellitus, where activation of the renin-angiotensin-aldosterone system, the beta-adrenergic system, oxidative damage, and metabolic disorders induced by hyperglycemia are the major contributors [4]. This type of fibrosis is also found in the aged heart, idiopathic dilated cardiomyopathy, and left ventricular pathology secondary to chronic aortic valve stenosis and regurgitation. Interstitial fibrosis is a marker of severity since it has been found in hypertensive cardiomyopathy, and it precedes irreversible replacement fibrosis [14].

### **Infiltrative Interstitial Fibrosis**

It is much rarer and is caused by the progressive deposition of insoluble proteins (amyloidosis) or glycosphingolipids (Anderson-Fabry disease) in the cardiac interstitium. Their pathophysiology is similar, and early detection of cardiac involvement is of critical importance for therapeutic management [15, 16].

### **Replacement Fibrosis**

Replacement fibrosis is caused by the replacement of damaged or necrotic myocytes by plexiform fibrosis mainly by type 1 collagen,

and is only seen when the integrity of the cell wall is compromised. Regional or localized (ischemic cardiomyopathy, myocarditis, hypertrophic cardiomyopathy, sarcoidosis) or diffuse (chronic renal failure, toxic cardiomyopathies, or various inflammatory diseases) patterns may exist depending on the underlying cause.

### Physics Bases of Magnetic Resonance

The protons in the body have an intrinsic electromagnetic charge, have a positive charge and are rotating on their own axis, their orientation is random and their magnetic fields cancel each other. By introducing protons into an intense and homogeneous electromagnetic field, most of them will align in the direction of the field (parallel) and others in the opposite direction (antiparallel), so that some of their magnetic fields will cancel, and the remainder will produce the “net magnetization”. MR images are the result of the signal emitted by protons from hydrogen atoms in the body. Due to its electric charge, the proton can present two types of movements: the magnetic movement or spin, consists of the rotation that the proton makes on its own axis, and the precession movement is defined as the rotation that the proton makes when adapting to the

magnetic field. external where we place it. The best atoms, from the point of view of nuclear magnetic resonance (NMR), are those with a spin of ½ because they are the easiest to observe and the ones that give clearest and, therefore, most useful signals.

Resonance is achieved by applying a radio frequency (RF) wave that matches the precession frequency of the proton we want to excite. Said precession frequency can be calculated with the Larmor formula, in which the precession frequency is equal to the intensity of the magnetic field measured in Teslas multiplied by the gyromagnetic constant that is measured in Hertz/Tesla, in this case the precession frequency for Hydrogen it is defined as 42 MHz/T, therefore, the precession frequency in a 1.5T resonator will be 64 MHz (Table 1) [17]. That is, the frequency with which nuclear spins precess depends on the intensity of the applied magnetic field (the greater the field, the greater the speed of rotation) and the particular nucleus in question (Table 1). We see that H is the one with the greatest gyromagnetic constant, and, therefore, the most sensitive to NMR.

**Table 1: Magnetic properties of different nuclei.**

Núcleo	Abundancia isotópica %	Spin	$\gamma / (10^7 T^{-1} s^{-1})$	$\nu_L / \text{MHz en un campo de 2,35 T}$
<sup>1</sup> H	99,985	1/2	26,7522	100,0
<sup>2</sup> H	0,015	1	4,1066	15,35
<sup>13</sup> C	1,10	1/2	6,7283	25,14
<sup>14</sup> N	99,634	1	1,9338	7,22
<sup>15</sup> N	0,366	1/2	-2,7126	10,13

*Fuente: Giménez Martínez y Expósito López, RMN para Químicos Orgánicos.*

Excitation phase: When a radio frequency pulse excites a set of protons, the result will be that at room temperature the protons in phase will form a net magnetization vector. This pulse must cease in an instant of time to allow the sample to return to equilibrium, getting rid of this excess energy and after that a relaxation phase will occur. (17) relaxation phase. Once the radiofrequency pulse is over, the protons return to their normal position, in this recoil there is also a release of energy in the form of radiofrequency captured by the antenna for imaging.

### T1 relaxation (longitudinal)

By applying a 90° radiofrequency pulse, it is possible to rotate the longitudinal magnetization to the transverse plane, so that the longitudinal magnetization at this moment is 0, later the magnetization grows again in the longitudinal direction, which we call longitudinal relaxation or T1. The time in which the different tissues return to their longitudinal magnetization is different in each one, and this is what provides us with the contrast. T1 is a parameter that is specific for each tissue and also depends on the intensity of the electromagnetic field. The definition of T1 is the time in which

the longitudinal magnetization reaches 63% of its final value, after an RF pulse of 90°.

### T2 relaxation (transverse)

When applying a 90° radiofrequency pulse, the net magnetization aligns in the transverse plane, however the protons begin to get out of phase with each other due to various factors. When the phase shift is due to the effect called “spin – spin interaction”, it can also be called “T2 decay” or “T2 relaxation”. When the transverse magnetization is completely in phase, that is when we have the largest MR signal, the signal begins to decrease while the phase shift occurs, and is zero when the phase phase is complete. The T2 is a characteristic parameter of each tissue and characterizes the time in which the protons of a tissue are out of phase. The definition of T2 is the time in which the transverse magnetization decays by 37% [17].

The magnetic resonance image is fundamentally determined by the density of the voxels and by the pulse sequence to which the voxels under study are subjected, as well as by the repetition time

or TR (time in which the pulse sequences are repeated at throughout the acquisition of the image) and by the echo time or TE (time elapsed between the excitation of the H nuclei and the refocusing of the signal once the extension of the TE has been defined). This concludes that short TE and TR (TE < 60 ms and 400 < TR < 800 ms) produce T1-weighted images, and long TE and TR (TE > 70 ms and TR > 2000 ms) create T2-weighted images. The foregoing will allow the creation of T1-weighted images, when fat appears hyperintense and fluids appear hypointense. On T2-weighted images, fluids appear hyperintense.

### Investment-recovery

It is a useful sequence to suppress the signal of a specific tissue in an MRI (hyperintense fluid, hypotense fat). Contrast weighting can be controlled by selecting TR and TE. A 180° radiofrequency pulse is performed prior to the regular sequence; the 180° pulse causes a reversal of the longitudinal magnetization. When the tissue signal to be suppressed crosses the 0 axis, a second 90° RF pulse is applied that rotates the other tissue signals to the transverse plane. Since the tissue signal is on the 0 axis, it does not present a signal, so it does not contribute to the brightness of the image. Inversion time (TI) is the time between the initial 180° RF pulse and the second 90° pulse.

### Cardiac MRI

Cardiac magnetic resonance imaging is a well-established method and is considered the gold standard for the assessment of myocardial volumes and function, as well as for the quantification of myocardial fibrosis in ischemic and non-ischemic heart disease.

### T1 mapping

T1 mapping consists of quantifying the longitudinal relaxation time of a tissue using analytical expressions of image-based signal intensities. The T1 relaxation time between two tissues varies substantially, with edema, fat, and fibrosis having different relaxability. The T1 time of a tissue can act as a marker to assess the extent of myocardial damage, for which specific sequences based on inversion-recovery are used to determine the longitudinal recovery rate.

### Technique for obtaining T1 maps

The T1 mapping sequence is acquired in a single apnea. There are multiple varieties of the basic inversion recovery sequence including Look-Locker (LL), Modified Look-Locker (MOLLI) and sequences derived from it as shortened MOLLI. For its evaluation, it is preferred to obtain short axes in 3 slices to increase the volume of the sample. The pulse sequences used for the measurement of myocardial T1 times require cardiac synchronization methods to freeze cardiac motion. In general, the investment-recovery sequence is used [18].

### Look-Locker

The LL sequence is performed continuously and prospectively throughout the cardiac cycle, without concern for myocardial motion or any specific method of cardiac synchrony. A 180° pulse

is applied and images are obtained at different ITs. Images in LL are obtained in a single long breath hold (20-28 seconds). She is always referred to as LL or “T1 Scout” [1, 4].

### Soft

To overcome the limitations of LL sequences, he developed a new technique that allows the selective acquisition of information in a single part of the cardiac cycle (end-diastole) in a series followed by heartbeats. MOLLI is a technique consisting of 3 sets of Look – Locker experiments with 3 heartbeats (or 3 seconds) between them to ensure magnetization recovery, this method is performed in a single apnea (16 – 20 seconds). Each of the 3 experiments start with an inversion pulse given a specific TI, after which single-shot images are acquired on consecutive beats.

All images are acquired with the same end-diastolic delay time, with an acquisition time of 191 msec. The 3 series (of 3, 3 and 5 images) result in a set of 11 source images, which are identical except for the reversal time. By merging these images into a data set, the values for each pixel are analyzed by computer, it is then that a map can be generated [4].

### Goal

#### general objective

- Determine the reference values of myocardial T1 relaxation times in our population to justify their clinical interpretation in the tissue evaluation of different cardiovascular diseases.

#### Specific objectives

- Evaluate the distribution of myocardial T1 relaxation times in the study population.

### Materials and Methods

#### study design

We designed the research study as a cohort, prospective, and single-center study.

#### Patient selection

The study was approved by the Ethics Committee of the Faculty of Medicine, UNAM. Written informed consent was obtained from all participants. 27 healthy volunteer subjects were included (the sample size complies with the recommendations to acquire reference values in native mapping). Some of the volunteers were recruited from the workers of the CT Scanner Mexico center. All potential volunteers participated in an interview and clinical examination. to rule out possible cardiovascular disease, following the guidelines of the modified Framingham Risk Score [19].

#### Inclusion Criteria

Patients with no significant cardiovascular history, with an age range between 25 to 69 years, with no history of medical treatment for cardiovascular or chronic-degenerative diseases. Blood pressure, HR, and Sat O2 were taken, and clinical parameters such as age, sex, body mass index, psychobiological habits, and important personal or family history were recorded. In addition to the para-

metric mapping techniques, a standardized imaging protocol was performed for the evaluation of cardiac function and chamber size, continuing with the mapping sequences for subjects without evidence of structural abnormalities, with LVEF and normal cardiac diameters. Four groups were established: <34 years, 35-44 years, 45-54 years and > 55 years.

### Exclusion Criteria

Volunteers with any condition that could directly or indirectly alter cardiac morphology and function were excluded. These included patients with known heart disease (coronary artery disease, cardiomyopathies, myocarditis, arrhythmias, etc.), chronic degenerative diseases (systemic arterial hypertension, diabetes mellitus, history of CVD, COPD, asthma), pulmonary thromboembolism, pulmonary hypertension, renal disease, chronic and any malignant or rheumatic disease, peripheral arterial disease, morphological abnormalities on MRI, and contraindications to MRI study (implantable devices, brain aneurysm clips, cochlear implants, severe claustrophobia).

### Cardiac Magnetic Resonance Protocol

All images were acquired in a 1.5 Tesla resonator (Siemens Magnetom Aera, Siemens Healthineers, Erlangen, Germany). A 3-lead vectored cardiogram was used for electrocardiographic triggering. The procedure was performed with the patient in the supine position, during inspiratory apnea and without movement of the chest or abdomen during image acquisition. Protocols included CINE Steady State Free Precession (SSFP) sequences in 2-chamber, 3-chamber, and 4-chamber views. For T1 mapping, 3 short-axis slices were acquired in the basal, middle, and apical position of the left ventricle. The size of the field of view (FOV) was 360 mm. Electrocardiographic triggering was used to acquire images in systole.

For T1 mapping, the MyoMaps tool based on the MOLLI technique was used. The flight resolution was 1.4 X 1.4 mm, the slice thickness was 8 mm with an interslice space of 16 mm, TR was 2.7 msec, TE 1.13 msec, TI 180msec and vector inclination of 35°, matrix 144 X 256. These parameters are consistent with the recommendations for optimizing MOLLI T1 acquisition [19].

### Image analysis

All the series of images were analyzed by 2 observers, the author of the thesis, and verified by a specialist in cardiovascular imaging with 9 years of experience. Post-processing was performed using commercially available software dedicated to cardiovascular imaging (cvi42, version 5.11, Circle Cardiovascular Imaging Inc., Calgary, Canada). Evaluation of ventricular volumes and function, as well as T1 mappings, was performed.

### T1 mapping analysis

Evaluation of T1 values was performed using equipment-generated T1 maps (grayscale or color) from magnetic resonance imaging in 3 short-axis slices located in the basal, middle, and apical third (Figure 1). Landmarks were then placed at the junction sites between the right and left ventricle to define left ventricular myocardial segmentation according to the American Heart Society (AHA) (Figure 2). Semi-automated contouring of the endocardial and epicardial borders of the left ventricle (Figure 3) was performed using the “Click-Draw Contours” tool of the software, with 10% exclusion of the segmented endocardial and epicardial borders to reduce the volume effect. The T1 relaxation time of the blood pool was obtained by placing an ROI in the center of the myocardial cavity in the basal third. The mean relaxation times were recorded for each slice and for each of the AHA myocardial segments (Figure 4) (1-16).

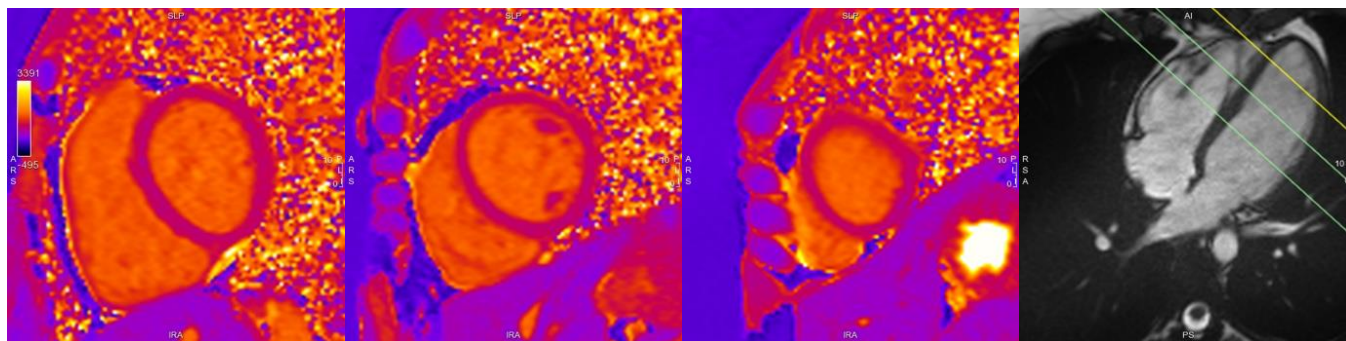


**Figure 1:** T1 maps in basal, mid and apical slices and reference image.

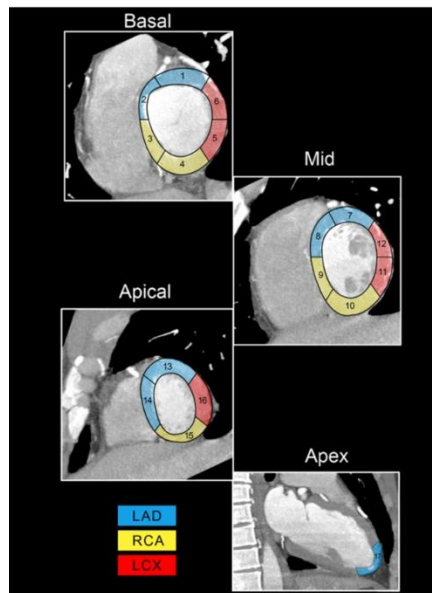


**Figure 2:** Myocardial segmentation and vascular territories. (Image obtained from StatDx)

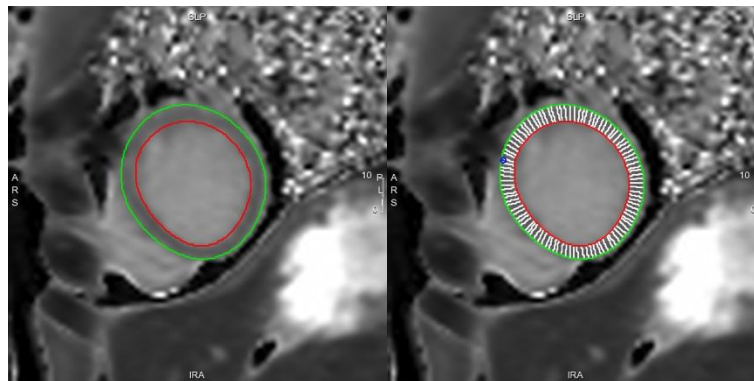


**Figure 3:** Example of endocardial and epicardial border contouring. The contours are represented in red (endocardial) and green (epicardial). A 10% compensatory erosion was applied to both contours to reduce partial volume effects, with the final area of interest represented in white.

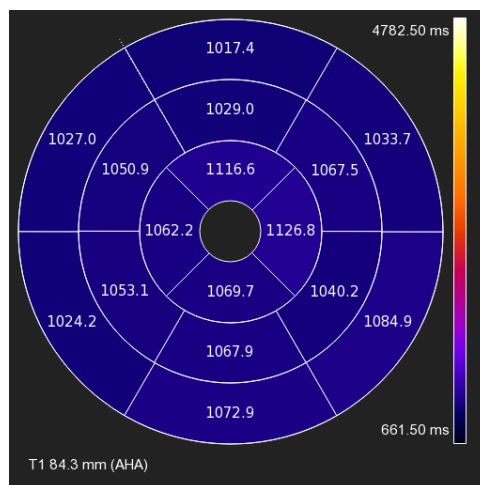


**Figure 4:** Mean T1 relaxation times per myocardial segment.

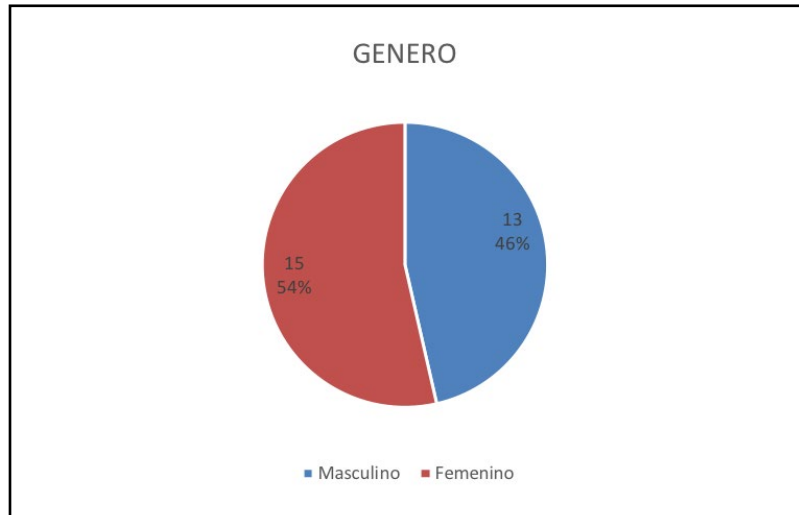
### Statistic analysis

Once the data was captured in Excel (Microsoft), the SPSS (IBM) software was used for the mathematical characterization of the variables, and the information was analyzed with descriptive statistical techniques. The descriptive characteristics of the study participants were analyzed as mean, standard deviation, median, minimum and maximum values, and percentiles. Percentages were used for the categorical evaluation of some variables (sex and age group). This analysis will seek to account for the frequencies that were reported for each variable. A global quantile regression analysis, adjusted for age and sex, was used to assess the distribution of longitudinal relaxation values.

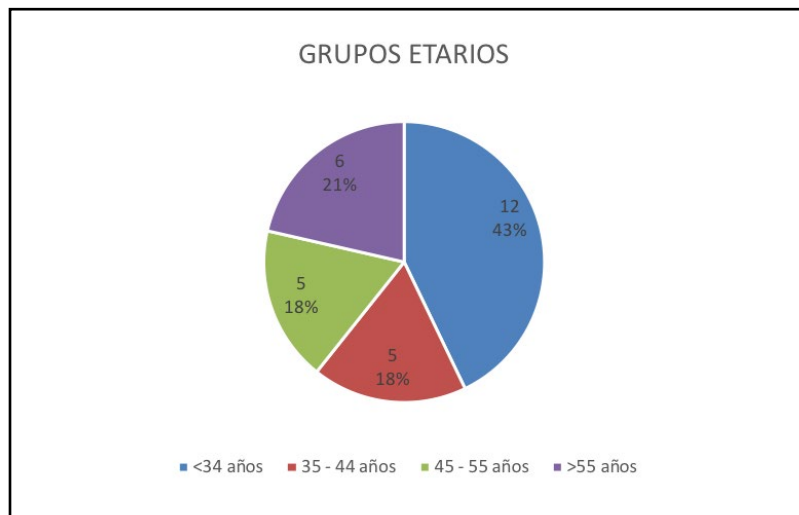
### Results

#### Participant characteristics

The study included 28 healthy volunteers, of whom 15 were women (53% and 13 were men (47%) (Graph 1). One patient was excluded due to severe claustrophobia. The mean age was 41.5 years (SD 13.2) with a range from 25 to 69 years, which was stratified into 4 groups: < 34 years, 35-44 years, 45-54 years and > 55 years (Graph 2). Six participants (21%) had active smoking or a history of it. A table is presented with demographic values, cavity diameters, left and right ventricular function, complete with the sample of participants (Table 2).



Graph 1: Distribution of the sample by gender



Graph 1: Distribution of the sample by age group

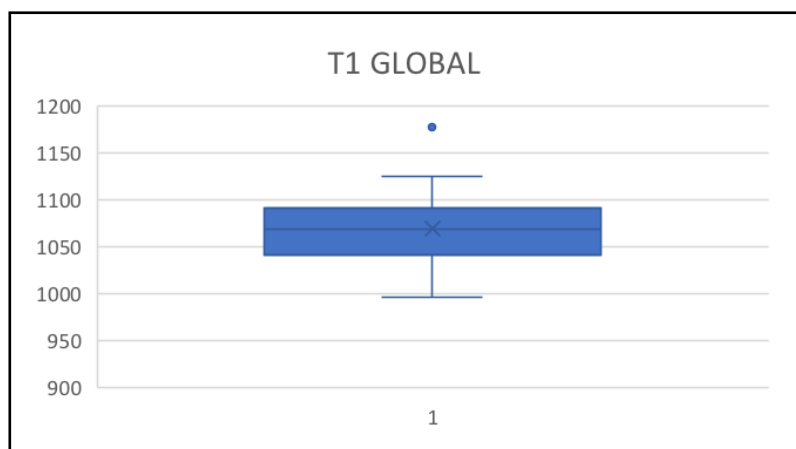
**Table 2: Characteristics of the study participants.**

	N	Media	Mediana	DE	Mínimo	Máximo	Percentiles		
							25	50	75
<b>EDAD</b>	28	41.54	39	13.287	25	69	30	39	51
<b>PESO</b>	28	67.36	65	12.434	47	90	58.5	65	79.5
<b>TALLA</b>	28	165.18	162	9.137	151	180	159.25	162	174.75
<b>FC</b>	24	72.46	73	8.382	52	89	67.25	73	77
<b>DDVI</b>	28	44.07	46	5.298	32	52	40	46	47.75
<b>SIVD</b>	28	7.5	7	2.028	3	12	6	7	8
<b>PPD</b>	28	6.82	7	1.611	4	10	6	7	8
<b>DSVI</b>	28	27.11	27.5	4.323	17	35	23.5	27.5	29.75
<b>FEVI</b>	28	63.04	61	6.42	49	77	59	61	68
<b>VTD</b>	28	105.46	106.5	24.358	60	167	85	106.5	122.75
<b>VTS</b>	28	39.46	39	12.351	18	66	29.5	39	46.75
<b>VLVI</b>	28	66	64.5	14.974	33	101	57.5	64.5	76.5
<b>MASAVI</b>	28	78.21	74.5	21.074	50	125	60.25	74.5	93.75
<b>FEVD</b>	28	53.46	53.5	9.469	37	74	46.5	53.5	60.75
<b>VTDVD</b>	28	102.07	99	26.316	52	167	82.25	99	123.75
<b>VTSVD</b>	28	47.39	44	13.75	26	81	38	44	55
<b>VLVD</b>	28	55.68	55.5	17.261	30	85	39.25	55.5	69

**T1 Mapping Results**

The mean global myocardial T1 value was 1069.41 ms with a SD of 38.73 ms. The distribution of the values is summarized in Graph 3. Among the age groups, the group <34 years had the lowest global T1 values. (1057 SD 33 msec), and the 35-44 year old group obtained the highest values (1100 SD 50 msec), so no direct relationship was found between the linear increase in age and the variability of relaxation times. Between both sexes, men had lower global T1 values than women (1049 vs 1086). The distribution of T1 times in the different age and gender groups are shown in Graphs 4 and 5.

Taking myocardial segmentation into account, the average myocardial T1 times were calculated in the basal, mid, and apical short-axis slices, observing a progressive increase in times as we approached the apex, obtaining an average of 1048 ms in the slice basal, 1064 ms in the middle cut and 1094 ms in the apical cut (Graph 6). Likewise, the averages of each of the AHA segments were obtained, also identifying an increase in times as the apical third progresses (Graph 7).

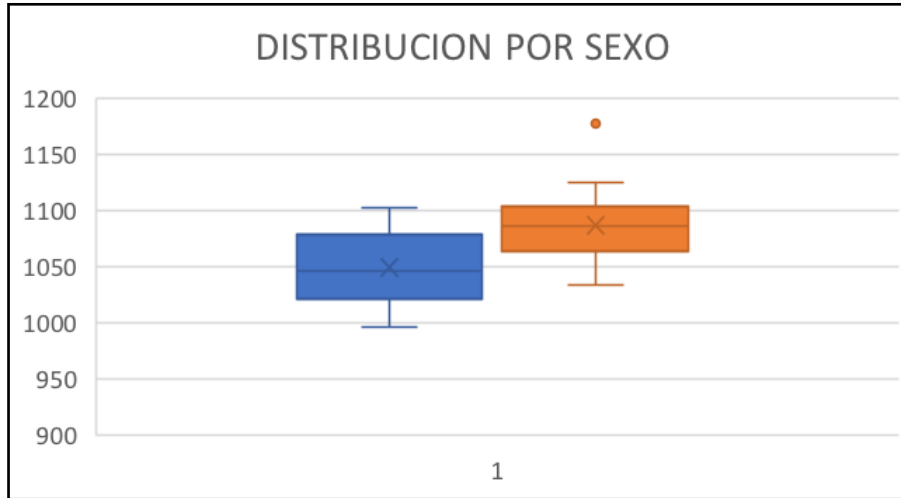


**Graph 3: Global myocardial T1 value.**

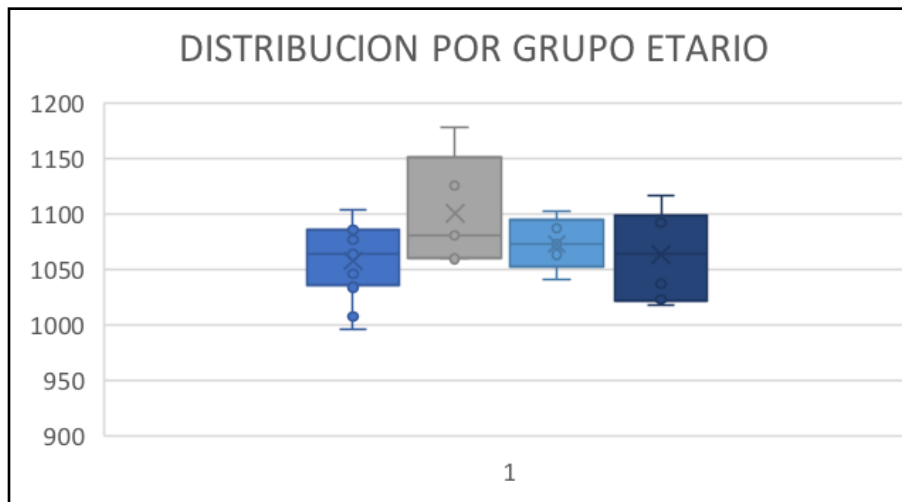


**Table 3: Average values of global myocardial T1 in the population groups (age and sex).**

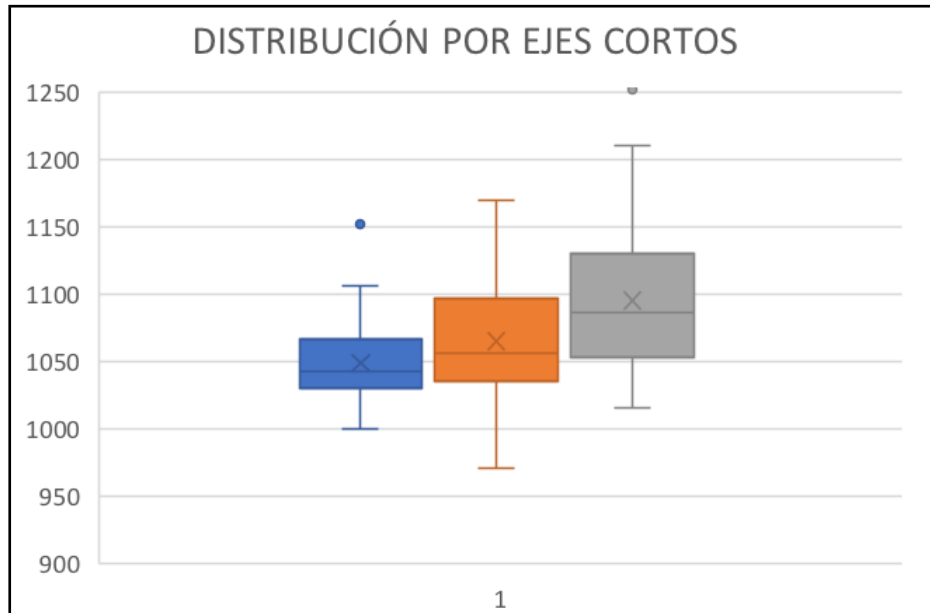
GRUPOS	< 34 años	35-44 años	45-54 años	>55 años	Hombres	Mujeres
MEDIA (MS)	1057.77778	1100.6	1073.333332	1063.44444	1049.38462	1086.77778
MEDIANA (MS)	1064	1080.666667	1073.33333	1064.5	1045.66667	1085.66667
DE (MS)	33.544282	50.74303455	23.20560313	42.1909241	32.8088872	35.7117354
MÍNIMO(MS)	996.333333	1059.666667	1041	1018.33333	996.333333	1034
MÁXIMO(MS)	1103.66667	1177.666667	1102	1117	1102	1177.66667



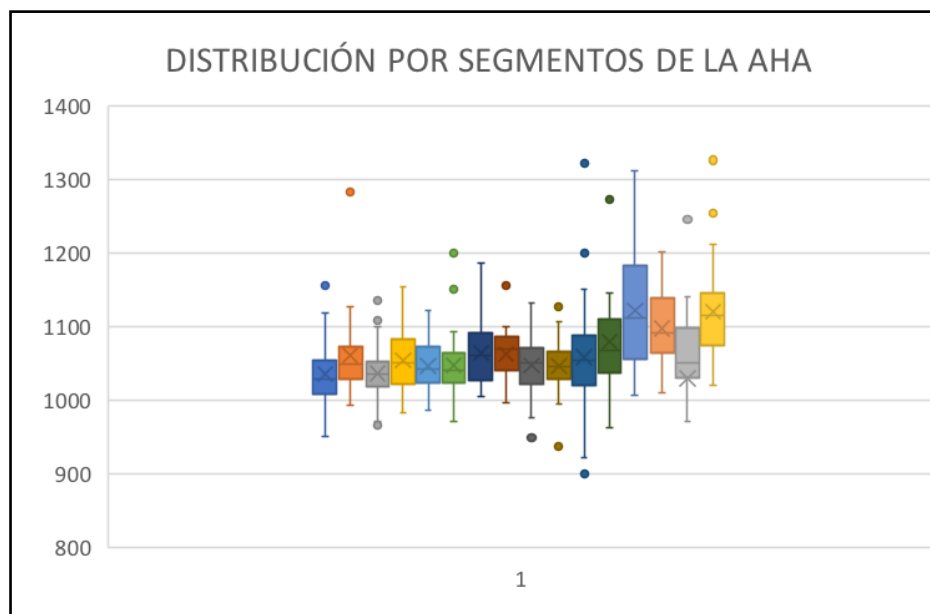
**Graph 4:** Distribution of global myocardial T1 times by sex (blue=men, orange=women)



**Graph 5:** Distribution of global myocardial T1 times by age groups (blue color codes <34 years, gray 34-44 years, turquoise 45-54 years, navy >55 years)



**Graph 6:** Distribution of myocardial T1 times in basal, mid, and apical slices of the left ventricle (blue=basal, orange=medium, gray=apical)



**Graph 7:** Distribution of myocardial T1 times in the AHA segments (ordered from segment 1 to 16)

### Discussion

The latest guidelines published by the European Association of Cardiovascular Imaging (AEICV) published in 2017(20), recommend the determination of T1 times locally with subsequent correlation with the data already published, however it is mentioned that for clinical use it should be use the local reference. There are several works that have investigated the longitudinal relaxation times of the myocardium of the healthy population, without cardiovascular disease, however none of them includes patients with the racial or geographical characteristics of our population [21, 10, 7]. Therefore, we consider that we have presented the only database of myocardial T1 relaxation times carried out in a healthy

Latin American population, and it is a fundamental need for its subsequent comparison with studies in populations with similar characteristics. Likewise, it will allow obtaining the value of correlation and use as a diagnostic tool in the evaluation of diffuse and segmental myocardial diseases. Most of the variation that can be obtained in these values is the result of the partial volume effect (reduced, when performing the erosion of the endo and epicardial borders) and the intensity of the electromagnetic field, observing in other studies a significant difference in time when using 1.5 and 3 T resonators, so it is not useful to transpolate our results in the studies acquired in 3T equipment, and the result of the partial volume effect [22]. In studies carried out in 1.5 T equipment, native

T1 times have been obtained that vary between 950 ms and 1034 ms. We have shown that myocardial native T1 is a robust parameter with a narrow normal range, so its reproducibility is possible; however, for its clinical use, studies with the same specifications and conditions are required to obtain the values. reference.

### Conclusions

Cardiac MRI is becoming increasingly important in the detection of myocardial diseases, due to tools such as late enhancement and mapping techniques. The latter help us to assess the myocardium quantitatively, since the information obtained during the acquisition and represented in the voxels is much greater than what is visible to the human eye. Mapping techniques have advanced rapidly in the course of the last 15 years, and that is why the need to standardize their clinical use is becoming increasingly urgent.

The MOLLI sequence allows the quantification of these times in a reproducible way. The normal ranges of native T1 can serve as a basis for the quantitative characterization of the myocardium in the context of diffuse diseases, in patients with infarcts, storage diseases and inflammatory diseases. We are getting closer to standardizing clinical use, and the intention of this study was to go one step further for its use in the Latin American population.

### References

1. Hamlin, S. A., Henry, T. S., Little, B. P., Lerakis, S., & Stillman, A. E. (2014). Mapping the future of cardiac MR imaging: case-based review of T1 and T2 mapping techniques. *Radiographics*, 34(6), 1594-1611.
2. Sanz, J., LaRocca, G., & Mirelis, JG (2016). Myocardial mapping with cardiac magnetic resonance: diagnostic value of the new sequences. *Spanish Journal of Cardiology*, 69 (9), 849-861.
3. Salerno, M., & Kramer, C. M. (2013). Advances in parametric mapping with CMR imaging. *JACC: Cardiovascular imaging*, 6(7), 806-822.
4. Burt, J. R., Zimmerman, S. L., Kamel, I. R., Halushka, M., & Bluemke, D. A. (2014). Myocardial T1 mapping: techniques and potential applications. *Radiographics*, 34(2), 377.
5. Piechnik, S. K., Ferreira, V., Lewandowski, A. J., Ntusi, N., Sado, D., Maestrini, V., ... & Robson, M. D. (2012). Age and gender dependence of pre-contrast T1-relaxation times in normal human myocardium at 1.5 T using ShMOLLI. *Journal of cardiovascular magnetic resonance*, 14(1), 1-2.
6. Piechnik, S. K., Ferreira, V. M., Lewandowski, A. J., Ntusi, N. A., Banerjee, R., Holloway, C., ... & Robson, M. D. (2013). Normal variation of magnetic resonance T1 relaxation times in the human population at 1.5 T using ShMOLLI. *Journal of Cardiovascular Magnetic Resonance*, 15, 1-11.
7. Dabir, D., Child, N., Kalra, A., Rogers, T., Gebker, R., Jabbour, A., ... & Puntmann, V. O. Valores de referencia para el miocardio humano sano utilizando una metodología de T1 mapping: Resultados del Estudio Multicéntrico Internacional T1 de resonancia magnética cardiovascular.
8. Nacif, M. S., Turkbey, E. B., Gai, N., Nazarian, S., Van Der Geest, R. J., Noureldin, R. A., ... & Bluemke, D. A. (2011). Myocardial T1 mapping with MRI: comparison of Look-Locker and MOLLI sequences. *Journal of Magnetic Resonance Imaging*, 34(6), 1367-1373.
9. Munoz, C. G., Saldarriaga, C. I., & Martínez, J. D. (2019). Fibrosis miocárdica: hacia una nueva aproximación. *Revista colombiana de cardiología*, 26(3), 142-151.
10. Böttcher, B., Lorbeer, R., Stöcklein, S., Beller, E., Lang, C. I., Weber, M. A., & Meinel, F. G. (2021). Global and Regional Test-Retest Reproducibility of Native T1 and T2 Mapping in Cardiac Magnetic Resonance Imaging. *Journal of Magnetic Resonance Imaging*, 54(6), 1763-1772.
11. Sado, D. M., Flett, A. S., & Moon, J. C. (2011). Novel imaging techniques for diffuse myocardial fibrosis. *Future Cardiology*, 7(5), 643-650.
12. Mewton, N., Liu, C. Y., Croisille, P., Bluemke, D., & Lima, J. A. (2011). Assessment of myocardial fibrosis with cardiovascular magnetic resonance. *Journal of the American College of Cardiology*, 57(8), 891-903.
13. Schaper, J., & Speiser, B. (1992). The extracellular matrix in the failing human heart. In *Cellular and molecular alterations in the failing human heart* (pp. 303-309). Steinkopff.
14. Weber, K. T., & Brilla, C. G. (1991). Pathological hypertrophy and cardiac interstitium. Fibrosis and renin-angiotensin-aldosterone system. *Circulation*, 83(6), 1849-1865.
15. Shah, K. B., Inoue, Y., & Mehra, M. R. (2006). Amyloidosis and the heart: a comprehensive review. *Archives of Internal Medicine*, 166(17), 1805-1813.
16. Zarate, Y. A., & Hopkin, R. J. (2008). Lysosomal storage disease 3. *Lancet*, 372, 1427-1435.
17. Pooley, R. A. (2005). Fundamental physics of MR imaging. *Radiographics*, 25(4), 1087-1099.
18. Burt, J. R., Zimmerman, S. L., Kamel, I. R., Halushka, M., & Bluemke, D. A. (2014). Myocardial T1 mapping: techniques and potential applications. *Radiographics*, 34(2), 377.
19. Messroghli, D. R., Moon, J. C., Ferreira, V. M., Grosse-Wortmann, L., He, T., Kellman, P., ... & Friedrich, M. G. (2017). Clinical recommendations for cardiovascular magnetic resonance mapping of T1, T2, T2\* and extracellular volume: a consensus statement by the Society for Cardiovascular Magnetic Resonance (SCMR) endorsed by the European Association for Cardiovascular Imaging (EACVI). *Journal of Cardiovascular Magnetic Resonance*, 19(1), 1-24.
20. Messroghli, D. R., Moon, J. C., Ferreira, V. M., Grosse-Wortmann, L., He, T., Kellman, P., ... & Friedrich, M. G. (2017). Clinical recommendations for cardiovascular magnetic resonance mapping of T1, T2, T2\* and extracellular volume: a consensus statement by the Society for Cardiovascular Magnetic Resonance (SCMR) endorsed by the European Association for Cardiovascular Imaging (EACVI). *Journal of Cardiovascular Magnetic Resonance*, 19(1), 1-24.
21. Piechnik, S. K., Ferreira, V., Lewandowski, A. J., Ntusi, N., Sado, D., Maestrini, V., ... & Robson, M. D. (2012). Age and gender dependence of pre-contrast T1-relaxation times in normal human myocardium at 1.5 T using ShMOLLI. *Journal of*

---

cardiovascular magnetic resonance, 14(1), 1-2.

22. Dabir, D., Child, N., Kalra, A., Rogers, T., Gebker, R., Jabbour, A., ... & Puntmann, V. O. Valores de referencia para el miocardio humano sano utilizando una metodología de T1 mapping: Resultados del Estudio Multicéntrico Internacional T1 de resonancia magnética cardiovascular.

**Copyright:** ©2023: Nelsy Gonzalez Ramirez, et al. This is an open-access article distributed under the terms of the Creative Commons Attribution License, which permits unrestricted use, distribution, and reproduction in any medium, provided the original author and source are credited.